Journal of Alloys and Compounds 483 (2009) 573–577

Contents lists available at ScienceDirect

Journal of Alloys and Compounds

journal homepage: www.elsevier.com/locate/jallcom

Electrochemical characterization of platinum nanoparticles stabilized by amines

E. Ramírez-Meneses[a,*], M.A. Domínguez-Crespo[a], V. Montiel-Palma[b], V.H. Chávez-Herrera[a], E. Gómez[c], G. Hernández-Tapia[d]

[a] Centro de Investigación en Ciencia Aplicada y Tecnología Avanzada, CICATA-IPN Unidad Altamira, Km 14.5 Carretera Tampico-Puerto Industrial, C.P. 89600 Altamira, Tamaulipas, Mexico
[b] Centro de Investigaciones Químicas, Universidad Autónoma del Estado de Morelos, Av. Universidad 1001, Colonia Chamilpa, C.P. 62201 Cuernavaca, Morelos, Mexico
[c] Instituto de Química-Universidad Nacional Autónoma de México, Ciudad Universitaria, C.P. 04510 México, D.F., Mexico
[d] Gerencia de Catalizadores y Proceso, Instituto Mexicano del Petróleo, Eje Central Lázaro Cárdenas norte 152, 07730 México, D.F., Mexico

ARTICLE INFO

Article history:
Received 30 August 2007
Received in revised form 27 July 2008
Accepted 5 August 2008
Available online 17 November 2008

Keywords:
Nanostructured materials
Chemical synthesis
Electrochemical reactions
Transmission electron microscopy

ABSTRACT

In this work we present the synthesis by Chaudret approach of Pt nanoparticles stabilized by primary amine (–NH_2) compounds. Their electrochemical performance as cathodes in low temperature polymer electrolite fuel cells on the oxygen reduction reaction (ORR) is also presented. Transmission electron microscopy (TEM) images of the samples show Pt nanostructures with particle size varying from 10 to 100 nm depending on the kind of the stabilizer used during the catalyst preparation. In some cases well-dispersed isolated platinum nanoparticles were observed. The activity of the dispersed catalysts (Pt/C) with respect to the ORR was investigated using steady state polarization measurements. The kinetic parameters showed that although no significant differences between the Tafel slopes of the Pt catalysts exist, transfer coefficients and exchange current densities show higher activities when the Pt nanoparticles were stabilized by tert-butylamine (TBA). The performance with respect to the ORR of the Pt/C catalyst on vulcan carbon substrate is active and comparable to that reported in the literature for state-of-art electrocatalysts.

1. Introduction

Platinum supported on high surface area carbon substrates is still the most widely used electrocatalyst in low temperature polymer electrolyte fuel cells (PEMFCs), particularly for the cathode reaction [1]. While the overpotential for the oxidation of pure hydrogen (anode reaction) is negligible even at high current densities due to very facile H_2 oxidation kinetics on platinum, the strong kinetic inhibition of the cathodic oxygen reduction reaction (ORR) leads to high overpotentials, amounting to several hundreds of millivolts under typical PEMFC operating conditions [1]. Therefore, optimization of the Pt catalysts performance throughout new synthesis routes is needed. For this a large catalytic active surface area is required, which is typically achieved by having the noble metal nanoparticles small and well dispersed on an electron conducting support material with a large surface area. Several methods have been developed to synthesized platinum nanoparticles including salt reduction technique [2], where a wide range of reducing agents (such as alcohols [3], borohydrides [4,5], hydrazine [6] or dihydrogen [7]) have been used with good results in size and dispersion. However, the contamination on the surface of the obtained nanoparticles due to some of the employed reducing agents is an important disadvantage of this method. An interesting alternative to obtain "clean surface" nanostructured materials has been proposed by Chaudret and co-workers [8]; who have studied the coordination properties of different ligands on metal nanoparticles. They established from a series of experiments the predominant role of chemical equilibrium between all potentially coordinating agents (ligands resulting from the precursor, solvent and stabilizers) and concluded on their important effect over the size, shape and dispersion of the generated nanoparticles. They also mentioned that these materials can be obtained free of possible surface contamination. Recently, the same authors have reported interesting results on the obtention of Pt nanoparticles from $Pt_2(dba)_3$ as metallic precursor and hexadecylamine as stabilizer [9]. However, up to now, synthesis of Pt nanoparticles stabilized by amines from organometallic precursors for electrocatalysts is not found to best of scientist knowledge. In the present work we aim to investigate how the nature of different stabilizers containing amine group (–NH_2), such as tert-butylamine (TBA), $C(CH_3)_3NH_2$; 1,3-diaminopropane (DAP), $H_2N(CH_2)_3NH_2$, and anthranilic acid (AA), 2-$(H_2N)C_6H_4CO_2H$, modifies the size, shape and dispersion of Pt nanoparticles and their behaviour as cathode catalysts in the PEMFC. The ORR activities are measured

---

[*] Corresponding author.
E-mail address: esthervincent@yahoo.com (E. Ramírez-Meneses).

0925-8388/$ – see front matter © 2008 Elsevier B.V. All rights reserved.
doi:10.1016/j.jallcom.2008.08.141

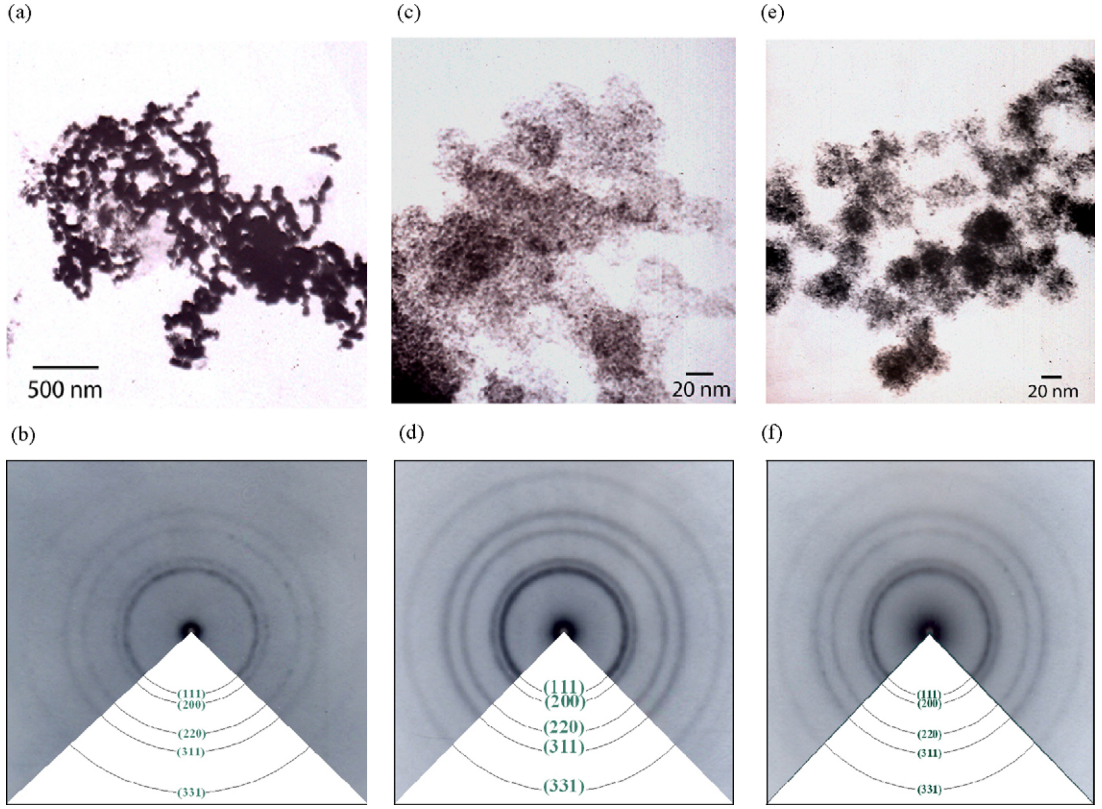

Fig. 1. Transmission electron micrographs and corresponding electron diffraction pattern of Pt-TBA (a and b), Pt-DAP (c and d) and Pt-AA (e and f) after the purification process.

and compared with those reported in the literature. Characterization by transmission electron microscopy (TEM) before fuel cell experiments was also performer in order to determine the nanosize distribution of the Pt particles.

2. Experimental

2.1. Synthesis of metallic nanoparticles

The platinum precursor, $Pt_2(dba)_3$, was prepared according to literature procedures [10] from K_2PtCl_4 (99.9%). The synthesis of nanoparticles was carried out as a standard procedure in a Fischer–Porter bottle at room temperature to obtain platinum colloids. Three different compounds were employed to stabilize platinum nanostructures; tert-butylamine, 1,3-diaminopropane and anthranilic acid according to the following experimental procedure: $Pt_2(dba)_3$ (0.036 mmol) was introduced in a Fisher–Porter bottle under argon atmosphere and 40 ml of THF distilled and degassed by freeze-pump cycles, was added. Thereafter, 0.6 mmol of tert-butylamine (98%) or 1,3-diaminopropane (99%) or anthranilic acid (98%) was added to the resulting violet solution. Then, the obtained dark brown solutions were pressurized under hydrogen atmosphere (3 bar) and after 20 h; a homogeneous black colloidal solution was obtained. During this time, the colloidal solutions were purified by hexane washings (to eliminate the dibenzylideneacetone). Finally, the resulting black solution was evaporated in vacuum until the residue was completely dry.

2.2. Catalysts preparation

The support of the electrode was a glassy carbon rod (5.0 mm in diameter). The base of the rod was polished with a cloth and alumina powder (ca. 0.3 μm). The working electrodes were prepared by attaching ultrasonically re-dispersed catalyst suspension containing a 4:1 ratio vulcan carbon black/total metal (20 wt.%) powders in deionized water onto the glassy carbon. After drying in flowing high purity argon at room temperature, the deposited catalyst layer was then covered with ≈4 μl of a diluted aqueous Nafion solution and finally, the electrode was immersed in nitrogen purged electrolyte to record the electrochemical measurements. The electrodes were carefully prepared in order to obtain reproducible electrode surfaces and comparable electrocatalytic results.

2.3. Electrochemical measurements

The electrochemical measurements were conducted via cyclic voltammetry (CV) and rotating disk electrode using a thermo stated standard three compartment electrochemical cell by means of an interchangeable ring-disk electrode setup with a bi-potentiostat and rotation control. 0.5 M H_2SO_4 was used as electrolyte. Before the electrochemical tests, the electrolyte was saturated with nitrogen gas for CV or oxygen gas for oxygen reduction. The counter electrode was a Pt grid and the reference electrode a reversible saturated calomel electrode (0.2415 V vs. RHE) connected to the working electrode compartment via Lugging capillary. The cyclic voltammograms were measured in the range from −0.50 to 1.3 V (vs. RHE) and the scan rate was 50 mV s^{-1}. All the specimens were analyzed until 50 cyclic potential scans in order to produce clean surfaces. The steady state polarization measurements were recorded in the range from −0.1 to 1.3 V vs. RHE at different rotation rates 400, 800, 1200, 1500 and 2000 rpm at a scan rate of 5 mV s^{-1}.

2.4. Characterization

Specimens for TEM analysis were prepared by slow evaporation of a drop of each colloidal solution after purification process deposited onto a holey carbon covered copper grid. TEM experiments were performed on a JEOL-1200 EX electron microscope, operating at 120 KV.

3. Results and discussion

TEM analysis of Pt-TBA systems display agglomerate particles with an elongated shape, mean size between 80 and 100 nm (Fig. 1a). The corresponding selected area electron diffraction pattern (SAED) exhibits the diffraction peaks from (1 1 1), (2 0 0), (2 2 0), (3 1 1) and (3 3 1) planes of (FCC) Pt (Fig. 1b). On the other hand, TEM analysis of the Pt-DAP system shows the presence of well-dispersed small particles of spherical shape, mean size 5–8 nm (Fig. 1c). The corresponding SAED pattern also exhibits (1 1 1), (2 0 0), (2 2 0), (3 1 1) and (3 3 1) planes corresponding to (FCC) Pt (Fig. 1d). Finally, TEM image of the Pt-AA specimen depicts sponge-like particles, mean size 30–50 nm (Fig. 1e). These particles

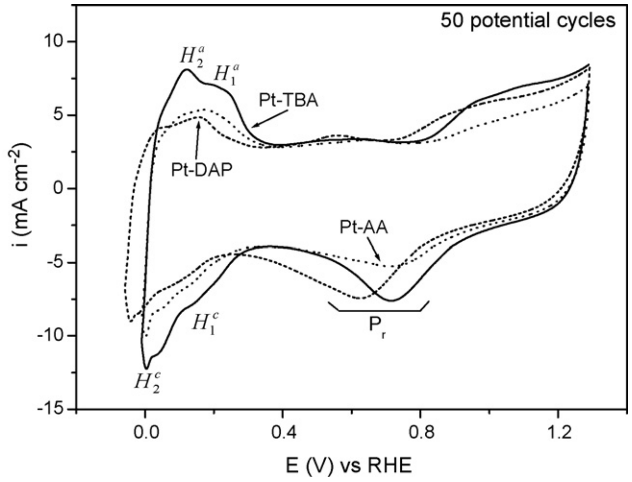

Fig. 2. Cyclic voltammograms after 50 potential cycles of different Pt catalysts obtained by organometallic method using different stabilizers at a sweep rate 50 mV s^{-1}.

result from the agglomeration of nanocrystallites. The corresponding SAED pattern confirms the presence of (FCC) Pt (Fig. 1f). It seems to be that Pt-DAP and Pt-AA nanoparticles are better dispersed than those of the Pt-TBA system. However, the particle sizes suggest that the synthesized system could be a suitable material for use in electrocatalysis.

Electrochemical properties of the ORR on the electrode electrocatalysts have been studied by analyzing rotating disk electrode (RDE) electrochemical data. The activation process of each sample was performed previously to the measurement, by scanning the cyclic voltammetry in the range of −0.1 to 1.3 V vs. RHE. Although the cyclic voltammograms of all catalysts reached a steady state after a few potential cycles, test were recorded up to 50 potential cycles to evaluate electrochemical stability of the samples, which were characterized by small pseudocapacitances between 0.4 and 1.3 V (Fig. 2). However, the shapes of the cyclic voltammograms were different based on the kind of stabilizer used during catalysts preparation. Fig. 2 also shows typical features of Pt and carbon surfaces after 50 potential cycles, with slightly less well-resolved H-adsorption–desorption peaks for the samples than those reported in the literature for Pt-ETEK [11,12]. Pt–OH peaks in the adsorption and desorption regions are distinct for each Pt catalysts, e.g., two anodic (desorption) and cathodic (adsorption) peaks H_1^a, H_2^a, H_1^c and H_2^c, respectively, can be distinguished for Pt-TBA and Pt-DAP, while in Pt-AA only one anodic peak is observed. In the hydrogen desorption region, the peak present at more negative potentials (H_2^a) is considered to be result of hydrogen desorption from the bulk of the metal together with the desorption of hydrogen adsorbed on the surface [13]. The peak obtained at more positive potentials (H_1^a) is attributed either exclusively to adsorbed hydrogen [14]. Changes in the amount of hydrogen desorbed manifested by the peaks H_1^a and H_2^a are proportional to the changes of the real surface area of the Pt-catalysts [15]. As it is observed, Pt-TBA shows the highest real surface area for this reaction. These curves also show a reduction peak (P_r) around 0.6 V; the peak is normally assigned to the electro-reduction of oxygen in Pt. It can be seen that the position of the current peak is shifted to a more positive value (i.e., lower overvoltage) when TBA and AA are used as stabilizers. The fact that the shape of the curves and displacement of the peaks (reduction of oxides/hydroxides) are modified by the stabilizer type indicates a modification in the form, size and dispersion of the Pt nanoparticles as was observed by TEM studies, which affects the electrochemical behaviour. In addition, it is difficult for the catalysts to be evaluated for their electrochemical stability based on the cyclic voltammograms shape. However, because the catalysts reached a steady state soon (only after 5 potential cycles), it can be considered that the catalysts are electrochemically stable.

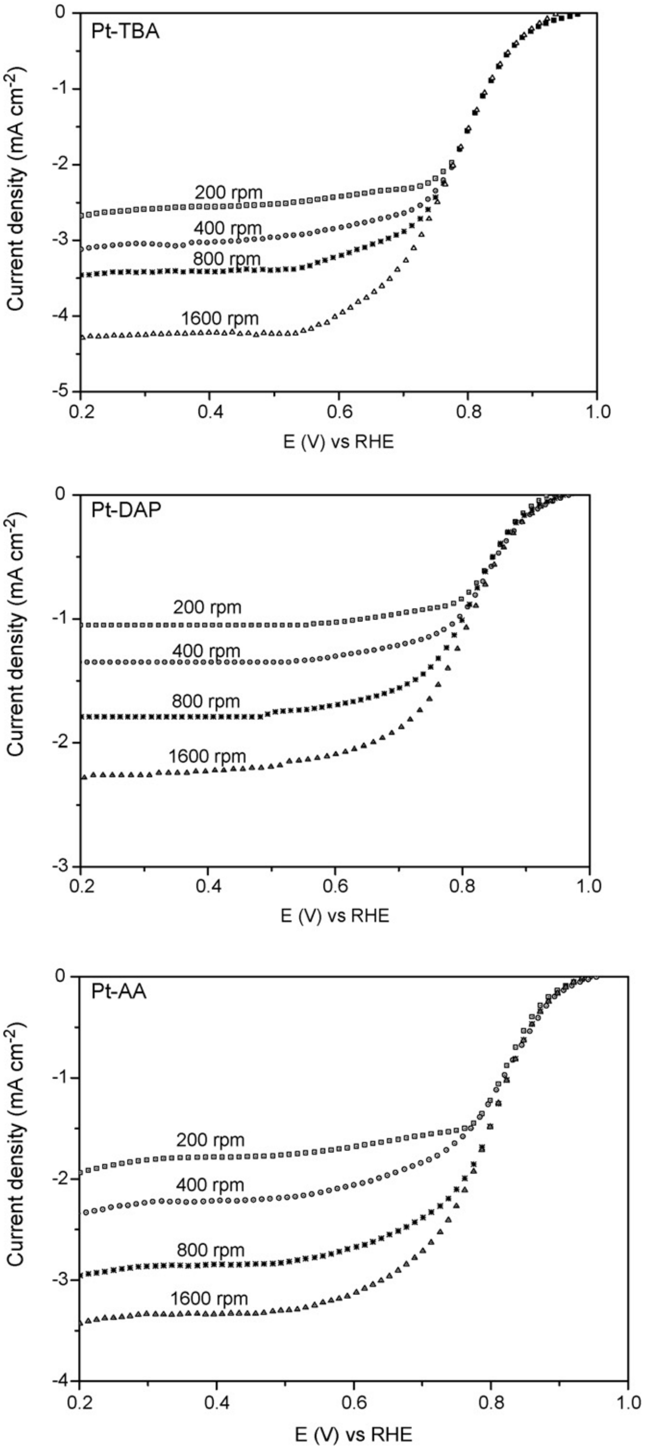

Fig. 3. Polarization curves for oxygen reduction reaction on different nanoparticles of Pt obtained from organometallic method using different stabilizers. (a–c) The Pt particles were dispersed into Nafion film on a glassy carbon electrode, in a O_2 saturated 0.5 M H_2SO_4 with a rotating geometric electrode area = 0.7 cm^2 and sweep rate = 5 mV s^{-1} at 298 K.

Current density potential curves at four different rotation rates produced by the molecular oxygen reduction at the Pt-catalysts incorporated into a Nafion film are shown in Fig. 3a–c. In all graph-

Table 1
Kinetic parameters obtained from the mass-corrected Tafel plots of the ORR in 0.5 M H_2SO_4.

Sample	Tafel slope ($-b$) (mV dec^{-1})	Transfer coefficient (α)	Log i_0 (mA cm^{-2})	i_1 $E = 0.9$ V (mA cm^{-2})	i_2 $E = 0.8$ V (mA cm^{-2})	i_3 $E = 0.75$ V (mA cm^{-2})
Pt-DAP	100 ± 4	0.56 ± 0.02	−4.1 ± 0.2	0.11 ± 0.01	0.70 ± 0.3	0.89 ± 0.2
Pt-AA	95 ± 2	0.59 ± 0.01	−4.4 ± 0.1	0.12 ± 0.02	0.98 ± 0.2	1.30 ± 0.3
Pt-TBA	84 ± 3	0.72 ± 0.01	−5.3 ± 0.2	0.26 ± 0.03	1.35 ± 0.1	1.86 ± 0.2

ics and results presented, the current density corresponds to the geometric area and was normalized to the Pt-loading in the electrodes. It can be noted on all catalysts that the ORR is diffusion controlled, when the potential is lower than 0.6 V vs. RHE and is under mixed diffusion-kinetic control between 0.6 and 0.8 V. Also, it is seen that the half-wave potentials are very similar for the three Pt-catalysts. The abrupt change in curvature observed at potential of 0.6 V corresponds to the limitations imposed by mass transfer. Differences between current densities can be associated with the kind of stabilizer used during catalysts preparation or an obstruction of active sites and the influence of the reduction area due to the liquid hydrocarbon used to prepare the carbon paste as it has been reported by other authors [16]. In the carbon paste electrodes, the resistance of the Nafion film which covers the supported catalysts is sufficiently small and the experimental catalytic current densities could be adjusted to the simple Koutechý–Levich first order reaction equation, without further need additional terms:

$$\frac{1}{i} = \frac{1}{i_k} + \frac{1}{i_d} \tag{1}$$

where i_k is the kinetic current density due to the charge-transfer at the electrode surface and i_d represents the diffusion limited current density, $i_d = B\omega^{0.5}$; ω is the angular frequency of rotation and B parameter is defined as $B = 0.2nFD_{O_2}^{2/3}\nu^{1/6}C_{O_2}$; n is the number of electrons transferred in the overall reduction process, F is the Faraday constant, D is the diffusion coefficient of the molecular oxygen, ν is the kinematic viscosity and C_{O_2} is the concentration of molecular oxygen [17–19]. Typical Koutechý–Levich plots (not shown) of the experimental values indicated that at high polarizations, slopes over a wide frequency interval can be fitted when the number of electrons transferred in the overall reduction process is four. Therefore, the limiting current densities observed for these materials follows a four-electron mechanism, i.e., $O_2 + 4H^+ + 4\bar{e} \rightarrow 2H_2O$, which has also seen in other works [16,20]. The electrocatalytic actives for the ORR on the Pt-catalysts were compared through mass transport corrected Tafel plots, as presented in Fig. 4. The catalytic activity towards the oxygen reduction reaction is higher when TBA is used as stabilizer. Pt catalysts obtained from DAP and AA displayed in the lower overpotential region similar behaviour with a slope close to -0.100 V dec^{-1} while in the high overpotential region ($E < 0.6$ V) a difference is observed in the current densities. The favourable effect obtained with TBA could be attributed to the elongated shape of the Pt nanoparticles observed by TEM studies, which have better electronic properties of the active centre and facilities the electron transfer. We believe that the presence of two NH_2 groups contained in DAP can give better stabilization to platinum nanoparticles because of the coordination of the amine groups on the surface but, at the same time, DAP could present less mobility of NH_2 group than that for TBA stabilizer. Therefore, the electroactivity in this reaction is influence by the mobility of NH_2 group. Finally, although Pt particles with AA as stabilizer showed agglomeration, its electroactivity is better than the Pt-DAP system. We suggest that the presence of AA, could possibly enhance the charge transfer phenomena due to the presence of the phenyl group in its structure and the likely coordination of the NH_2 moiety at the surface of the metallic particles. However, further analyses have to be carried out to confirm these hypotheses.

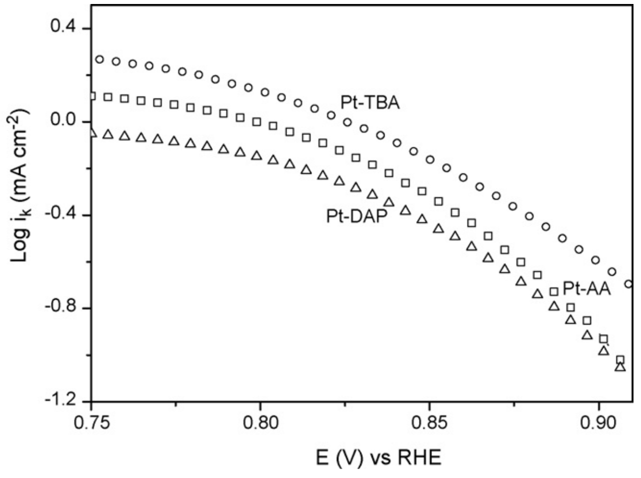

Fig. 4. Mass transfer corrected Tafel plots for Oxygen reduction on different nanoparticles of Pt dispersed into Nafion membrane in an O_2 saturated 0.5 M H_2SO_4.

The kinetic parameters deduced for the ORR on Pt-catalysts are shown in Table 1. These values are comparable with those published elsewhere [12,13]. It can be seen that although no significant differences exist between the Tafel slopes of the Pt catalysts, transfer coefficients and exchange current densities show higher activities when Pt nanoparticles were stabilized with TBA. This could indicate that the effect of the stabilizer is observed only in the effective area exposed. The electrochemical results suggest that Pt-catalysts synthesized from organometallic approach using a properly stabilizer could be considered as a good alternative in the fabrication of membrane electrode assemblies and for testing as a cathode for the ORR in a polymer electrolyte fuel cell.

4. Conclusions

The present study has shown that the nature of stabilizers influences shape, sized, dispersion and the electrocatalytic activity of the Pt nanoparticles when the organometallic approach is used. Therefore, the correct choice of these materials produces a synergistic interaction enhancing the electron transfer rate for the ORR. The electrochemical performance showed that Pt-catalysts prepared from TBA displayed higher activity than that showed when AA and DAP are used as stabilizers. Pt-TBA catalyst could be considered as a good alternative for its use as cathode in low temperature polymer electrolyte fuel cells.

Acknowledgements

The authors wish to acknowledge financial support and a M.Phil. grant (V.H.C.-H.) from IPN-Mexico (project SIP 20071254) and CONACyT (project 59921). We are also indebted to Mr. C. Flores-Morales (I.I. Materiales-UNAM) for TEM analysis.

References

[1] G. Schmid, M. Baümle, M. Geerkens, I. Heim, C. Osemann, T. Sawitowski, Chem. Soc. Rev. 28 (1999) 179.
[2] M.A. El-Sayed, Acc. Chem. Res. 34 (2001) 257.
[3] N. Toshima, Y. Yonesawa, N. J. Chem. 11 (1998) 1179.
[4] W. Yu, M. Liu, H. Liu, X. Ma, Z. Liu, J. Colloid Interf. Sci. 208 (1998) 439.
[5] M. Liu, W. Yu, H. Liu, J. Mol. Catal. A: Chem. 138 (1999) 295.
[6] Z. Liu, X. Lin, J. Yang Lee, W. Zhang, M. Han, L. Ming Gan, Langmuir 18 (2002) 4054.
[7] H. Bonnemann, G. Braun, W. Brijoux, A. Schlze Tilling, K. Seevogel, K. Siepen, J. Organomet. Chem. 520 (1996) 143.
[8] (a) B. Chaudret, Actualité Chimie 290–291 (2005) 33;
(b) A. Rodriguez, C. Amiens, B. Chaudret, M.-J. Casanove, P. Lecante, J.S. Bradley, Chem. Mater. 8 (1996) 1978;
(c) F. Dassenoy, K. Philippot, T.O. Ely, C. Amiens, P. Lecante, E. Snoeck, A. Mosset, M.-J. Casanove, B. Chaudret, N. J. Chem. 22 (1998) 703;
(d) S. Gomez, L. Erades, K. Philippot, B. Chaudret, V. Chem. 566 (2004) 281;
(e) C.O. Balmes, J.-O. Bovin, Chem. Commun. (2001) 1474;
(f) M. Gomez, K. Philippot, V. Collière, P. Lecante, G. Muller, B. Chaudret, N. J. Chem. 27 (2003) 114.
[9] E. Ramirez, L. Eradès, K. Philippot, P. Lecante, B. Chaudret, J. Adv. Funct. Mater. 17 (2007) 2219.
[10] K. Moseley, P.M. Maitlis, J. Chem. Soc., Chem. Commun. (1971) 982.
[11] K. Wikander, H. Ekstrôm, A.E.C., Palmqvist, G. Lindbergh, Electrochim. Acta. 52 (2007) 6848.
[12] I. Ávila-García, M. Plata-Torres, M.A. Domínguez-Crespo, C. Ramírez-Rodríguez, E.M. Arce-Estrada, J. Alloy Compd. 434–435 (2007) 764.
[13] A. Czerwinski, J. Electroanal. Chem. 379 (1994) 487.
[14] A.N. Correia, L.H. Mascaro, S.A.S. Machado, L.A. Avaca, Electrochim. Acta 42 (1997) 493.
[15] A. Czerwinski, Pol. J. Chem. 69 (1995) 699.
[16] R.L. McCreery, in: A.J. Bard (Ed.), Electroanalytical Chemistry, vol. 17, Marcel Dekker, New York, 1991.
[17] J. Perez, E.R. Gonzalez, E.A. Ticianelli, Electrochim. Acta 44 (1998) 1329.
[18] S. Durón, R. Rivera-Noriega, P. Nkeng, G. Poillerat, O. Solorza-Feria, J. Electroanal. 566 (2004) 281.
[19] Y.V. Pleskov, V.Y. Filinovskii, The Rotating Disk Electrode, Plenum Press, New York, 1976.
[20] R.R. Adzic, in: J. Lipkowski, P.N. Ross (Eds.), Electrocatalysis, vol. 5, VCH, New York, 1998, p. 197.